https://doi.org/10.5194/egusphere-2023-403
Preprint. Discussion started: 29 March 2023

Molecular signatures and formation mechanisms of particulate matter (PM) water-soluble chromophores from Karachi (Pakistan) over South Asia

Jiao Tang[1], Jun Li[1], Shizhen Zhao[1], Guangcai Zhong[1], Yangzhi Mo[1], Hongxing Jiang [2], Bin Jiang[1], Yingjun Chen[2], Jianhui Tang[3], Chongguo Tian[3], Zheng Zong[4], Jabir Hussain Syed[5], Jianzhong Song[1], Gan Zhang[1]

[1]State Key Laboratory of Organic Geochemistry and Guangdong province Key Laboratory of Environmental Protection and Resources Utilization, Guangdong-Hong Kong-Macao Joint Laboratory for Environmental Pollution and Control, Guangzhou Institute of Geochemistry, Chinese Academy of Sciences, Guangzhou, 510640, China

[2]Shanghai Key Laboratory of Atmospheric Particle Pollution and Prevention (LAP[3]), Department of Environmental Science and Engineering, Fudan University, Shanghai 200433, China

[3]Key Laboratory of Coastal Environmental Processes and Ecological Remediation, Yantai Institute of Coastal Zone Research, Chinese Academy of Sciences, Yantai, 264003, China

[4]Department of Civil and Environmental Engineering, Hong Kong Polytechnic University, Hong Kong, 999077, China

[5]Department of Meteorology, COMSATS University Islamabad (CUI), Islamabad, 45550, Pakistan

Corresponding Authors:

Jun Li: junli@gig.ac.cn; Gan Zhang: zhanggan@gig.ac.cn

https://doi.org/10.5194/egusphere-2023-403
Preprint. Discussion started: 29 March 2023

Abstract.

Excitation-emission matrix (EEM) fluorescence spectroscopy has been widely used to characterize chemical components of brown carbon (BrC), yet the molecular basics and formation mechanisms of chromophores decomposed by parallel factor (PARAFAC) analysis are not fully understood. Here, water-soluble organic carbon (WSOC) in aerosols from Karachi, Pakistan, were characterized with EEM spectroscopy and Fourier transform ion cyclotron resonance mass spectrometry (FT-ICR MS). Three PARAFAC components were identified, including two humic-like (C1 and C2), and one protein-like (C3) species. Among them, the C2 shows the longest emission maxima (~494 nm), and correlates tightly with the mass absorption efficiency at 365 nm (MAE_{365}), the character of BrC. Molecular families associated with each of the three components were determined by Spearman correlation analysis between FT-ICR MS peaks and PARAFAC component intensities. The C1 and C2 components are associated with nitrogen-enriched compounds, despite that C2 more with higher aromaticity, higher N content, and highly oxygenated compounds. The formulas associated with C3 include fewer nitrogen-containing species, with a lower unsaturated degree and oxidation state. A dominant oxidation pathway for the formation of C1 and C2 components was suggested, notwithstanding their different precursor types. A large number of formulas associated with C2 were found to be located in the "potential BrC" region, overlapped with BrC-associated formulas, and readily correlated tightly with MAE_{365}. This suggests that the compounds illuminating C2 may have also contributed substantially to the BrC light absorption. These findings were important for future studies using the EEM-PARAFAC method to explore the compositions, processes, and sources of atmospheric BrC.

https://doi.org/10.5194/egusphere-2023-403
Preprint. Discussion started: 29 March 2023

1. Introduction

Water-soluble organic carbon (WSOC), containing aromatic rings or aliphatic structures with carboxyl, hydroxyl, carbonyl, or methoxy functional groups, constitutes a significant portion of organic aerosols (OA) and can affect the roles of aerosols in climate processes, air quality, and human health (Lin and Yu, 2011; Wang et al., 2020b). Atmospheric WSOC originated from primary emissions, including biomass burning, coal burning, and other primary sources (Park and Yu, 2016; Li et al., 2018; Tang et al., 2020); as well as the secondary formations, such as the aqueous-phase reaction from anthropogenic or biogenic emission (Gilardoni et al., 2016; Lamkaddam et al., 2021; Updyke et al., 2012; Yu et al., 2021). Light-absorbing WSOC is an important component of brown carbon (BrC) and has a strong wavelength-dependent absorption that peaks in the ultraviolet (UV) spectral region and declines through the visible spectral region (Choudhary et al., 2022; Hecobian et al., 2010; Laskin et al., 2015; Sullivan et al., 2022). This fraction can contribute significantly to the global radiation balance and affects the photochemistry of the atmosphere (Feng et al., 2013; Kirchstetter and Thatcher, 2012).

The reactivity and fate of WSOC are tightly linked to its chemical composition, yet isolating and characterizing the constitutive elements and structure of light-absorbing organic molecules from among an abundance of non-absorbing molecules in aerosols is a challenging task. Bulk optical measurements, such as UV−visible (UV−vis) absorption spectroscopy, is an efficient means of characterizing the light absorption properties of BrC (Wu et al., 2021; Hecobian et al., 2010). Excitation-emission matrix (EEM) fluorescence spectroscopy can be employed to quantify and characterize a subset of BrC chromophores that absorb certain wavelengths of light and re-emit a fraction of that energy as fluorescence, providing further insight into the origin, chemical property, and process information. EEM is often coupled with parallel factor (PARAFAC) analysis, which mathematically decomposes the fluorescence data into

https://doi.org/10.5194/egusphere-2023-403
Preprint. Discussion started: 29 March 2023

various components, such as humic-like (HULIS), protein-like components (PLOM), and so on (Chen et al., 2016b; Jiang et al., 2022c; Tang et al., 2020; Chen et al., 2021a). Due to its high detection sensitivity and chromophore-resolving ability, EEM spectroscopy has been widely used to track BrC chromophore variations in chamber experiments (Bianco et al., 2014; Lee et al., 2013; Vione et al., 2019), and in ambient BrC studies (Wu et al., 2019; Yue et al., 2019; Chen et al., 2021b). Despite widespread use, the molecular basics of atmospheric fluorescent chromophores are not fully understood. Ultrahigh-resolution Fourier transform ion cyclotron resonance mass spectrometry (FT-ICR MS) is a powerful tool facilitating the analysis of organic matter based on individual molecular formulas that can aid in the interpretation of molecular patterns across systems (Jiang et al., 2014; Mopper et al., 2007). Based on this technique, thousands of molecular formulas can be obtained, and basic structural features can be deduced (Song et al., 2019; Zeng et al., 2021).

The water-soluble fraction of total OC aerosol is commonly up to 70% (Li et al., 2020b; Wu et al., 2019; Mo et al., 2022). Although serval studies have combined fluorescence analysis and FT-ICR MS to characterize the atmospheric WSOC, few have focused on the molecular characteristics of fluorescent components (Su et al., 2021; Tang et al., 2020; Li et al., 2022). Hence, it is necessary to seek the molecular basis of water-soluble fluorescent components.

Due to the chemical complexity of fluorescent chromophores, the formation of these compounds may be complex and would be determined by the precursors and atmospheric conditions (OH radicals, O_3, NO_x, and so on). For example, Lee et al. (2013; 2014) demonstrated that ammonia vapor converts initially colorless *d*-limonene/O_3 secondary organic aerosol (SOA) into BrC material, yet the *d*-limonene/O_3+NH_3 brown material almost completely lost its ability to absorb visible radiation or fluoresce after irradiation. Conversely, Bianco et al. (2014) examined that tryptophan, tyrosine, and 4-phenoxyphenol in an aqueous solution after irradiation produced species with similar fluorescence properties as humic substances. Fan et al. (2020) found that PLOM

https://doi.org/10.5194/egusphere-2023-403
Preprint. Discussion started: 29 March 2023

components decomposed by PARAFAC analysis are quenching with O_3 aging, yet HULIS components exhibit a gradual increase with O_3 aging. Recently, results based on observations in the online EEM system showed a conversion process between highly-oxygenated and less-oxygenated HULIS under atmospheric oxidation (Chen et al., 2021a). However, studies on the molecular evidence were limited for the formation of fluorophore compounds, especially PARAFAC fluorescent components; it is also important to constrain the properties of BrC aerosols.

Here, we examined the FT-ICR MS and fluorescence spectroscopy for WSOC in aerosols from Karachi, Pakistan in South Asia. Karachi represents a typical urban setting with a variety of air pollution sources including industrial and vehicular emissions, dust storms, and sea salts (Khwaja et al., 2009). The objectives of this study are to obtain: (1) the molecular families associated with PARAFAC components by using Spearman analysis of FT-ICR MS peaks and PARAFAC component intensities; (2) the possible formation pathway of PARAFAC components based on their molecular formulas; and (3) the molecular-level correlation between BrC chromophores and PARAFAC components. The results obtained help to understand the composition and fate of PARAFAC components, which broadens the application of the EEM-PARAFAC method to characterize atmospheric BrC.

2. Materials and Methods

2.1. Sampling campaign

Total suspended particulate (TSP) samples were collected in Karachi (24°51′N; 67°02′ E) from 2 February 2016 to 27 January 2017, as described previously (Zong et al., 2020). Briefly, the sampling site is on the floor of an office building of a government agency (approximately 12 m in height) located at the west edge of the main district of Karachi (Fig. S1 in Supplement). No agricultural land, but some semiarid bushes, surround it. Samples were collected on glass fiber filters with a high-volume sampler (KC-1000, Longtuo) at a flow rate of 1.13 m^3 min^{-1}. Diurnal sampling (12/12 h; day:

https://doi.org/10.5194/egusphere-2023-403
Preprint. Discussion started: 29 March 2023

133 10:00 am−10:00 pm; night: 10:00 pm−10:00 am, local time) was carried out once a
134 week. In total, 96 samples were collected during the sampling campaign. All filters were
135 preheated at 450 °C for 6 h in a muffle furnace before sampling. After sampling, the
136 filters were folded and stored in a refrigerator (−20 °C) until further analysis. The
137 classification of seasons based on the air-mass trajectories contains pre-monsoon (Mar–
138 May), monsoon (Jun–Sep), post-monsoon (Oct–Nov), and winter (Dec–Feb), where
139 marine air masses were prevailing in the monsoon period and continental air masses
140 were popularly occurred in the other periods, as shown in Fig. 1. The meteorological
141 parameters over Karachi during sampling periods were provided in Table S1.

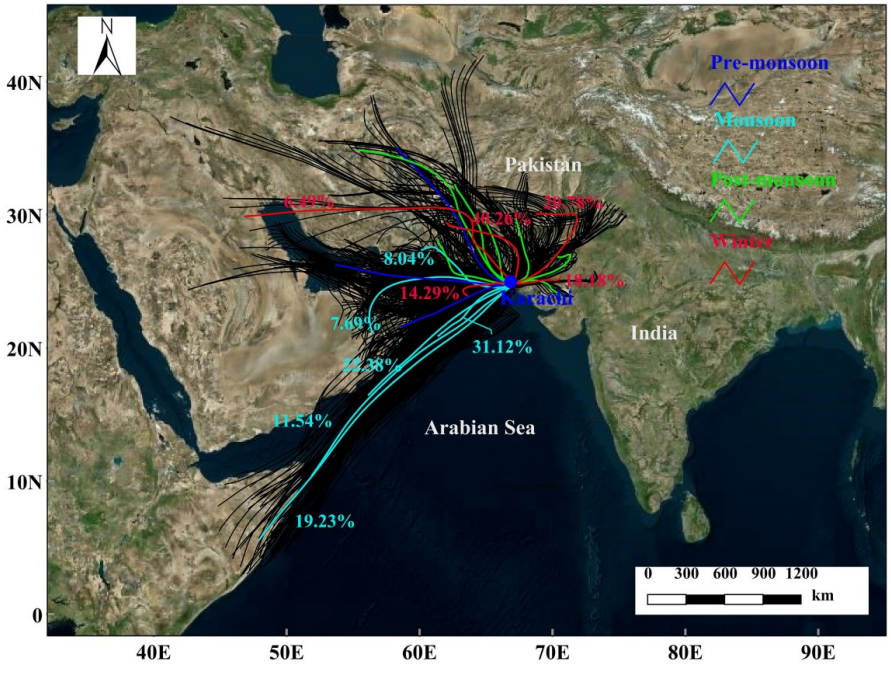

142

143 **Figure 1**. The 72 h back air-mass trajectories at Karachi (Pakistan) from February 2, 2016, to
144 January 27, 2017. The samples were classified into four seasons, whose air masses were further
145 conducted by the cluster analysis, including pre-monsoon (blue lines), monsoon (azure lines), post-
146 monsoon (green lines), and winter (red lines). The air-mass trajectories were analyzed by the
147 HYSPLIT model. The base map was derived from Bing Maps (© 2023 Microsoft).

https://doi.org/10.5194/egusphere-2023-403
Preprint. Discussion started: 29 March 2023

2.2. Optical characterization and PRAFAC modeling.

The detailed methods of fluorescence characterization and PARAFAC analysis have been described in our previous studies (Tang et al., 2021; Tang et al., 2020). Briefly, WSOC was obtained by ultrasonicating the filter punches in ultrapure deionized water (resistivity of > 18.2 MΩ) for 30 min and filtering the solutions. UV–vis absorption spectra and EEM spectra were simultaneously collected using a fluorometer (Aqualog; Horiba Scientific, USA). UV–vis absorption spectra were scanned in the range of 239 to 800 nm with a step size of 3 nm. Fluorescence scans were collected over increments of 3 and 4.66 nm for the excitation (239–800 nm) and emission (247–825 nm) wavelengths, respectively. The corresponding concentration of WSOC and water-soluble total nitrogen (WSTN) was quantified using a TOC analyzer (Vario TOC cube; Elementar) (Yu et al., 2017). The quality control for absorption spectra and EEM spectra, as well as carbon mass, were detailed in Text S1 of the supplement.

PARAFAC analysis was conducted to decompose the EEM datasets, using the drEEM Toolbox in MATLAB version R2016a (http://models.life.ku.dk/drEEM, last access: June 2014) (Murphy et al., 2013) (details in Text S2). The light absorption coefficient (Abs_λ, Mm^{-1}), mass absorption efficiency (MAE, $m^2\ g^{-1}$ C), absorption Ångström exponent (AAE), and optical indices, such as specific ultraviolet absorbance (SUVA), spectral slope (S_R), as well as fluorescence-based indices of the fluorescence index (FI), biological index (BIX), and humification index (HIX), were presented in Text S2.

2.3. FT-ICR-MS analysis.

A representative subset (12 samples) that covered a range of values of the relative intensities of PARAFAC components, WSOC concentrations, and total organic nitrogen at day and night in different seasons, was selected for ultrahigh-resolution electrospray FT-ICR MS analysis. Specially, the 72 h back air-mass trajectories of the selected samples showed different sources of air pollution (Fig. S2). Hence, the selected samples

https://doi.org/10.5194/egusphere-2023-403
Preprint. Discussion started: 29 March 2023

reflected the typical features during the sampling period. The sample preparation and analysis of FT-ICR MS are given elsewhere (Jiang et al., 2021; Tang et al., 2020). Briefly, the WSOC extracts were desalted and concentrated through the solid-phase extraction (SPE) method (Xu et al., 2020; Zhou et al., 2021), using a hydrophilic-lipophilic balance (HLB) cartridge (Oasis HLB, 200 mg/cartridge, Waters, USA) (Varga et al., 2001). The efficiency of the SPE method was evaluated by measuring the carbon masses, UV–vis, and EEM spectra before and after elution (Varga et al., 2001), which showed good analytical recoveries (details in Text S3). The majority of inorganic ions, low-molecular-weight (MW) organic acids, and sugars were not retained by the SPE, and the constituents retained on the SPE cartridge were eluted with methanol containing 2 % ammonia (v/v) (HPLC grade) (Lin et al., 2010). Methanol containing 2 % ammonia was selected for elution to reduce the mass percentage of irreversibly adsorbed carbon but not significantly change the molecular composition (Chen et al., 2016a; Lin et al., 2012a). The eluents were dried under a gentle nitrogen gas stream and redissolved in 1 mL of methanol for subsequent analysis.

Preceding FT-ICR-MS analysis, ultrahigh-resolution mass spectra were obtained using a solariX XR FT-ICR MS instrument (Bruker Daltonics GmbH, Bremen, Germany) equipped with a 9.4 T superconducting magnet and an electrospray ionization (ESI) ion source. Ions were produced in negative and positive ESI ion mode (hereinafter abbreviated as ESI– and ESI+). The ion accumulation time was set to 0.6, and the *m/z* range was set to 150–800. Peaks were considered if the signal-to-noise ratio was greater than 4. A typical mass-resolving power of > 450 000 at m/z 319 with < 0.2 ppm absolute mass error was achieved. The identified formulas were classified into subgroups (CHO–, CHON–, CHOS–, CHONS–, CHO+, CHON+, CHONa+, and CHN+). The CHO– and CHO+ refer to those that contain carbon, hydrogen, and oxygen and are detected in the ESI– and ESI+ modes, respectively. Other compound categories are defined analogously. Note that we report all detected compounds as neutral species unless stated otherwise. The double bond equivalent (DBE), modified aromaticity index

https://doi.org/10.5194/egusphere-2023-403
Preprint. Discussion started: 29 March 2023

(AI_{mod}), carbon oxidation state ($\overline{OS}_C$) and the nominal oxidation state of carbon (NOSC) are calculated in Text S4. The formulas were further classified into four categories referring to the AI_{mod} and H/C ratio (Kellerman et al., 2015; She et al., 2021): condensed aromatic compounds ($AI_{mod} \geq 0.67$); aromatic compounds ($0.5 < AI_{mod} < 0.67$); highly unsaturated and phenolic compounds ($H/C \leq 1.5$, $AI_{mod} \leq 0.5$); and aliphatic compounds ($1.5 \leq H/C \leq 2.5$).

2.4. Statistical analyses

The molecular families associated with each PARAFAC component were derived using Spearman correlation analysis according to our previous method (Jiang et al., 2022c). Before analysis, the PARAFAC component intensities were normalized to the total fluorescence intensity for a given sample, and the intensities of FT-ICR MS peaks were normalized to the total intensity of all peaks to which formulas were assigned within a sample. Then, Spearman's correlations between the FT-ICR MS and PARAFAC component data were conducted in R. Note that FT-ICR MS peaks that were present in fewer than two samples were not considered. For an n of 12 samples, a Spearman's coefficient (r_s) of 0.57 was calculated to be significant at the 95% confidence limit (Student's t test, see Text S5). When Spearman's $r_s \geq 0.57$, the molecule was assigned to the PARAFAC components. The same method was used to obtain the molecular signatures of PARAFAC components of dissolved organic matter (DOM) in aquatic environments (Stubbins et al., 2014; Singer et al., 2012). The molecular formulas associated with Abs at 365 nm (Abs_{365}), and optical indices (S_R, $SUVA_{254}$, A_{254}, FI, BIX, and HIX) were similarly obtained. Note that many of these associations may be due to different compounds responding in the same way to environmental conditions.

https://doi.org/10.5194/egusphere-2023-403
Preprint. Discussion started: 29 March 2023

3. Results and Discussion

3.1. Fluorescence and light absorption properties

PARAFAC analysis identified three individual fluorescent components (Fig. 2a), two humic-like (C1, C2), and one protein-like (C3) (Ishii and Boyer, 2012; Coble, 2007; Wu et al., 2019). All of them have been ubiquitously detected in aerosols (Wu et al., 2019; Wen et al., 2021; Wang et al., 2020a; Han et al., 2020), snow (Zhou et al., 2021), and rainwater (Li et al., 2020c). Based on the comparison with the EEM region of fluorescent components classified by a previous study (Chen et al., 2016b), C1, C2, and C3 were similar to less-oxygenated and highly-oxygenated HULIS, and non-N-containing components, respectively. Note that the origins and chemical properties of the components defined in this study are not necessarily similar to those of components with the same name in other organic matter.

The relative abundances of PARAFAC component intensities were used to indicate the changes in chemical compositions. Humic-like components (C1 and C2) were the dominant species of the whole-year samples, representing 80 %±6.1 % of total fluorescence intensity (Fig. S3), which is in accordance with precipitation samples in the Guanzhong basin of China while higher than that at Seoul (Yan and Kim, 2017; Li et al., 2022). Of those, C1 is 2-fold greater than that C2. During the sampling period, measurements of water extracts revealed the differences in PARAFAC component distributions in different seasons. When the monsoon is prevailing (marine-derived air masses, Fig. 1), the contribution of humic-like components decreased significantly (t-test, $p < 0.01$), suggesting that humic-like components may have a terrestrial origin. Recent work revealed that continental-influenced WSOC was enriched in aromatic and higher oxidation level compounds, while saturated primary marine biological compounds with lower oxidation levels were more abundant in marine-influenced WSOC (Mo et al., 2022). The redundancy analysis (RDA, detail in Text S6) conducted on PARAFAC components and noncollinear variables (variance inflation factors, VIF

https://doi.org/10.5194/egusphere-2023-403
Preprint. Discussion started: 29 March 2023

254 < 10) showed that C2 was positively related to HIX, A_{254}, and $SUVA_{254}$, and C1 was
255 positively associated with HIX, yet C3 correlated with FI, BIX, and S_R (Fig. S4). The
256 results reflected that C1 and C2 are associated with a high degree of humification and
257 aromaticity (Zsolnay et al., 1999; Weishaar et al., 2003).
258

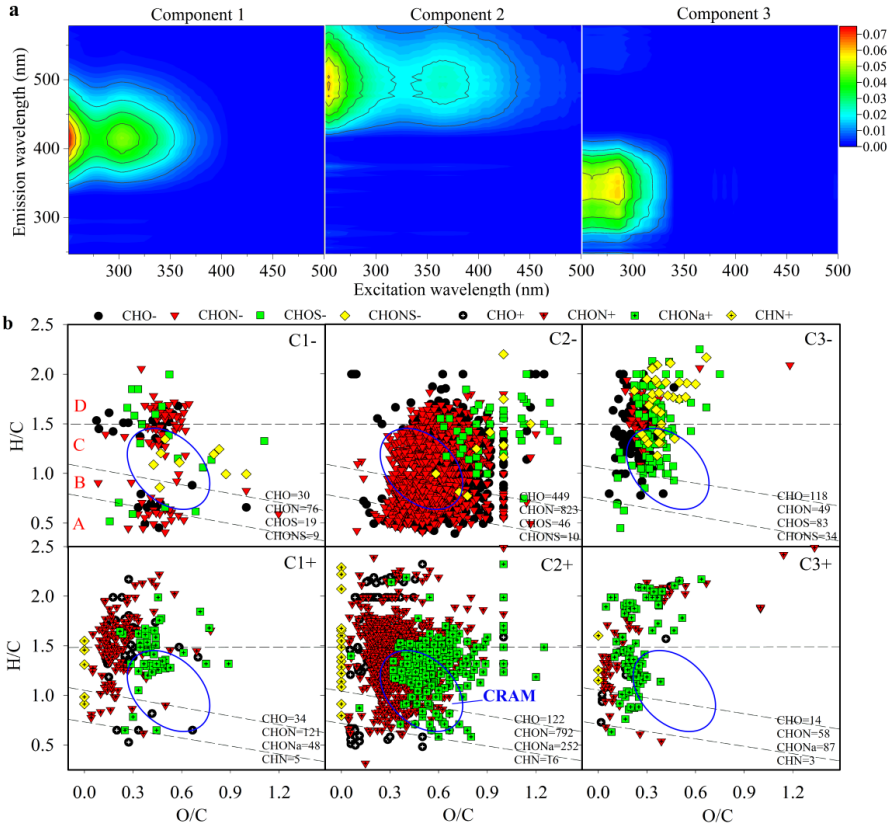

259
260 **Figure 2**. Molecular characteristics of PARAFAC components. (**a**) Patterns of the fluorescent
261 components (C1-3) identified by using the PARAFAC method. (**b**) van Krevelen diagrams of FT-
262 ICR MS-identified compounds assigned to PARAFAC components (C1, C2, and C3). C1- and C1+
263 refer to the molecules that are assigned to C1 detected in the ESI– and ESI+ modes, respectively,
264 and the others are defined analogously. Carboxylic-rich alicyclic molecules (CRAM) are remarked
265 by the blue ellipse (Hertkorn et al., 2006). The dotted line shows the class identification, including
266 condensed aromatic compounds (A); aromatic compounds (B); highly unsaturated and phenolic
267 compounds (C); and aliphatic compounds (D).

268 The mass absorption efficiency at a wavelength of 365 nm (MAE_{365}) is a key
269 parameter that can be used to describe the light-absorbing ability of the different

https://doi.org/10.5194/egusphere-2023-403
Preprint. Discussion started: 29 March 2023

chromophores in BrC. The MAE_{365} of water extracts in Karachi were 0.80±0.40 m^2 g^{-1} C, which is comparable to that in Kharagpur (India) (Srinivas and Sarin, 2014) and Godavari (Nepal) (Wu et al., 2019), higher than in Indo-Gangetic Plain (IGP) outflow, such as Northern region of Maldives and Bay of Bengal (Bosch et al., 2014; Srinivas and Sarin, 2013), yet much lower than other cities in South Asia (Table S2, and Fig. 3c). The values of MAE_{365} in monsoon daytime (nighttime) and non-monsoon daytime (nighttime) are 0.47±0.20 m^2 g^{-1} C (0.71±0.30 m^2 g^{-1} C) and 0.88±0.34 m^2 g^{-1} C (0.92±0.48 m^2 g^{-1} C), respectively (Fig. 3a). The MAE_{365} exhibited strong seasonal variation and was much higher at non-monsoon than in the monsoon (test-t, $p < 0.01$), potentially due to the different sources and formation process. However, considerably increasing MAE_{365} values during nighttime than daytime in monsoon were observed (t-test, $p < 0.05$), perhaps indicating that more light-absorbing substances were formed during nighttime $NO_3^{\cdot}$ reaction and significantly enhanced the light absorption capacity of BrC in monsoon (Li et al., 2020a). No obvious increase was observed in non-monsoon season (t-test, $p > 0.05$).

https://doi.org/10.5194/egusphere-2023-403
Preprint. Discussion started: 29 March 2023

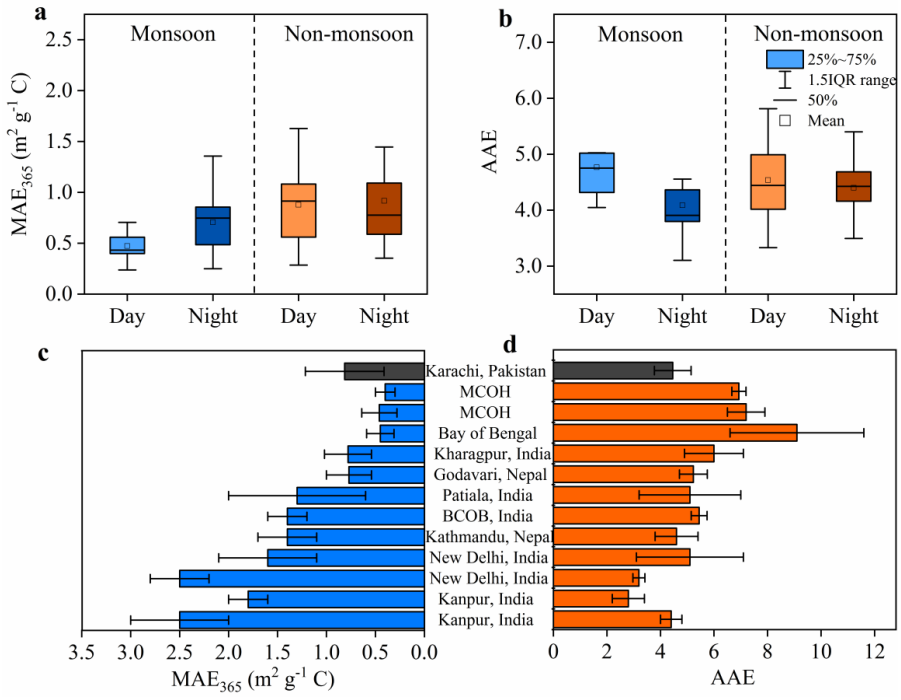

Figure 3. The seasonal and diurnal distributions of MAE_{365} (**a**) and AAE (**b**) of WSOC in Karachi, Pakistan. Panels **c** and **d** refer to the MAE_{365} and AAE of WSOC reported in recent studies over South Asia, including the Northern region of Maldives (MCOH) (Dasari et al., 2019; Bosch et al., 2014), Bay of Bengal (Srinivas and Sarin, 2013), Kharagpur (Srinivas and Sarin, 2014), Godavari (Wu et al., 2019), Patiala (Srinivas et al., 2016), Bhola Island in the delta of Bay of Bengal (BCOB) (Dasari et al., 2019), Kathmandu (Chen et al., 2020), New Delhi (Kirillova et al., 2014; Dasari et al., 2019), and Kanpur (Choudhary et al., 2018; Choudhary et al., 2021). The column marked in black color represents our results.

The parameter AAE reflects both the wavelength dependence of light absorption and the conjugated degree of the extracted compounds. The average AAE values (fitting at 330–400 nm) of WSOC in Karachi were very close in monsoon (4.4±0.85) and non-monsoon season (4.5±0.62) (Fig. 3b). However, the AAE values of WSOC during monsoon nighttime substantially decreased (t-test, $p < 0.05$), indicating a more aromatic and conjugated level of WSOC during nighttime, consistent with the significantly increased MAE values in this season. Except for in the IGP outflow, the AAE values of WSOC in Karachi were similar to that in South Asia, only higher than Kanpur and New Delhi (Fig. 3d). In addition, as humic-like components and MAE_{365} of WSOC

https://doi.org/10.5194/egusphere-2023-403
Preprint. Discussion started: 29 March 2023

significantly decreased in monsoon season and increased in non-monsoon season, the correlation between them was carried out (Fig. S5). The result showed that only C2 positively correlated with MAE_{365} ($r = 0.49$, $p < 0.01$), suggesting that C2, representing a category of compounds, potentially makes significant contributions to the BrC light absorption. To ascertain this preliminary conclusion, we further investigated the molecular composition of fluorescent chromophores, as discussed below.

3.2. Molecular signatures of PARAFAC components

Using Spearman's rank correlations at the 95 % confidence limit, 22 % of total ESI– formulas and 23 % of ESI+ formulas were assigned to the three PARAFAC components, respectively. The elemental formulas of each PARAFAC component are listed in Table S3, and the elemental composition characteristics of complex molecular formulas of PARAFAC components are presented by the Van Krevelen (VK) diagrams, as shown in Fig. 2b.

The C1 was assigned 134 ESI– formulas and 208 ESI+ formulas, in which only one formula overlapped in both modes. C1-assigned formulas were enriched in N-containing molecules, accounting for 63 % and 61 % of its assigned ESI– and ESI+ formulas, respectively. Of those, CHON was the most prevalent. Given that the C1-assigned formulas contain abundant nitrogen and are oxygenated ($\overline{OS}_C$, and NOSC) (Kroll et al., 2011), NO_x-derived reactivity could occur in the formation of this component (He et al., 2022; Lee et al., 2014). In contrast to C2 and C3, C1 formulas had middle elemental composition ratios (e.g., O/C, H/C, and N/C), oxidation state ($\overline{OS}_C$, and NOSC), as well as unsaturated degrees (AI_{mod}, and DBE) and relatively higher MW (Table S3, Figs. S6–S7). Of the formulas assigned to C1, 34 % of ESI– formulas and 50 % of ESI+ formulas were aliphatic compounds, 35 % and 39 % were highly unsaturated and phenolic compounds, and 31 % and 11 % were aromatic compounds.

https://doi.org/10.5194/egusphere-2023-403
Preprint. Discussion started: 29 March 2023

A larger number of 1328 ESI– formulas and 1182 ESI+ formulas were assigned to C2, of which 108 formulas were overlapped. In common with C1, 67 % of ESI– formulas and 68 % of ESI+ formulas contained nitrogen, suggesting that C2 is also an N-enriched component. However, C2 formulas contain two or more nitrogen compared with C1 (N atom ≥ 2, 38 % vs 14 % in ESI– and 42 % vs 18 % in ESI+) (Table S4), perhaps because they have different precursors or origins. For example, $CHON_2$ species are observed almost exclusively in the aged limonene ozonolysis sample than in *a*-pinene ozonolysis (Laskin et al., 2014). C2 with the longest emission maxima (~ 494 nm), was assigned to more compounds in higher aromaticity (AI_{mod} > 0.5), higher oxidation state ($\overline{OS}_C$ > 0), and higher N content (N/C > 0.2) (Fig. S6). Accordingly, the aromaticity index, N/C ratio, and NOSC correlated maxima with fluorescence in a pattern strikingly similar to C2 (Fig. S8), consistent with a previous study (Kellerman et al., 2015). Specially, C2 formulas contain more compounds in the region of carboxylic-rich alicyclic molecules (CRAM) that are represented by carboxylated and fused alicyclic rings with very few hydrogen atoms in double bonds, yet not common for C1 and C3, suggesting that C2 has a probable character of resistance to biodegradation and refractory nature (Hertkorn et al., 2006). The findings collectively indicated that C2 is a highly aromatic, oxygen-rich, and high N-content component, with potentially recalcitrant properties in the atmosphere.

Lower than 4 % ESI– and ESI+ formulas were assigned to C3. In contrast, more than 60 % of formulas contain no nitrogen atoms (Table S3), implying that the atmospheric protein-like component is not exclusively associated with N-containing compounds, consistent with previously reported (Stubbins et al., 2014). A possible explanation is that lignin, simple phenols, and naphthalene have a strong fluorescence signal in this region (Hernes et al., 2009; Maie et al., 2007; Wu et al., 2019). Of the formulas assigned to C3, almost all aromatic ESI– compounds and 43 % of aromatic ESI+ compounds are without nitrogen, suggesting that a portion of water-soluble protein-like components were substantially derived from N-free or N-depleted aromatic

https://doi.org/10.5194/egusphere-2023-403
Preprint. Discussion started: 29 March 2023

compounds, which corroborated the previous results (Chen et al., 2016b). However, an increasing fraction of S-containing species was observed, representing 41 % of C3-assigned ESI– formulas. Although these S-containing compounds may have no substantial contribution to BrC chromophores or fluorophores, similar formation pathways or origins is the potential to reflect C3 fate. C3 was strongly associated with less aromaticity degree ($AI_{mod} < 0.5$) and a higher degree of saturation compounds ($H/C > 1$) (Fig. S6), hence, lower than 5 % of formulas assigned to C3 were aromatic and condensed aromatic compounds. This character coupled with less oxidation state ($\overline{OS}_C < 0$, $O/C < 0.5$) collectively indicate that the atmospheric protein-like component is low conjugation, oxygen-depleted, and N-depleted species.

The use of Spearman's correlations purposefully allowed molecular formulas to correlate with one or more PARAFAC components as a given FT-ICR MS molecular formula can include many different structural isomers. Thus, the common molecules assigned to different PARAFAC components could preferentially reflect their similar chemical structures, molecular compositions, and origins. Of the formulas assigned to PARAFAC components, C1 shares 52 ESI– formulas and 42 ESI+ formulas with C2 (Fig. S9). The overlapped formulas represented 39% of 134 ESI– formulas and 20% of 208 ESI+ formulas assigned to C1. This observation indicates that C1 possesses a molecular-level correlation with C2, suggesting that they may have similar origins and atmospheric processes, as discussed below. However, no common molecules were found between C3 and C1 and C2, respectively.

3.3. Potential formation mechanisms of PARAFAC components

Early studies suggested that C1 and C2 components are less oxygenated and highly oxygenated humic-like components, respectively (Chen et al., 2016b), and another study found the two components may transform each other under atmospheric oxidation (Chen et al., 2021a). However, the formation pathways for these components are not fully understood. Conversely, fluorescence changes along with molecular composition

https://doi.org/10.5194/egusphere-2023-403
Preprint. Discussion started: 29 March 2023

were observed in the photolysis experiment of naphthalene-derived SOA (Lee et al., 2014). HULIS-type fluorescence was also found to be produced in the vanillin and acetosyringone solutions under simulated sunlight, attributed to oligomerization processes observed from their molecular composition (Vione et al., 2019). These results indicated that the molecular signatures could reflect possible formation pathways of fluorescent components. It is worth noting that the selected samples for FT-ICR MS analysis were collected on the day and night in different seasons, yielding a relatively complete molecular dataset, thus to better explain the formation pathways of fluorescent component-associated formulas we considered the potential precursors from the molecular dataset. The reason is that the precursors may be not associated with fluorescent components not as same as their formed new compounds, resulting in an underestimation of the contribution.

The molecular composition of PARAFAC components was determined, including CHO–, CHON–, CHOS–, CHONS–, CHO+, CHON+, CHONa+, and CHN+ compounds. For the different groups, the pathways may substantially differ. Given that the N-containing compounds were enriched, in particular for C1 and C2, the formation mechanism of this group was discussed first. N-containing compounds contain CHON– (CHONS– was classified as S-containing compounds), CHON+, and CHN+ (few were associated with PARAFAC components and no longer discuss). Of the CHON formulas assigned to PARAFAC components, the organic nitrogen molecules are suggested to be divided into the subgroups by using the O/N ratios, such as oxidized forms with O/N > 2 ($-NO_2$ or $-ONO_2$), reduced forms with O/N < 2 (amino or amide groups), which has been widely used for the classification of CHON molecules in FT-ICR MS studies (Mo et al., 2022; Jiang et al., 2022b; Zeng et al., 2021). A high relative abundance of CHON subgroups in aerosol samples appeared O/N ≥ 3, generally like to contain numerous oxidized nitrogen function groups (Mo et al., 2018). In this study, 87 % of CHON– and 74 % of CHON+ molecules assigned to C1, 84 % and 63 % of formulas assigned to C2, and 86 % and 33 % of formulas assigned to C3, had O/N ≥ 3 (Figs. 4a, 4b, 4c and S10a,

https://doi.org/10.5194/egusphere-2023-403
Preprint. Discussion started: 29 March 2023

S10b, S10c). Of those, the oxidized CHON assigned to C1 and C2 may be underestimated due to their formulas containing two-, and two more N atoms and need no 3 folds of O atoms to form $–NO_2$ or $–ONO_2$ groups. Hence, we assumed that these CHON formulas assigned to PARAFAC components were largely in an oxidized form.

Recent work summarized the several pathways for organic nitrates, including oxidation-product pair, hydrolyzation-product pair, mixed-processes product, and the remaining unknown product (Su et al., 2021). Kames et al. (1993) found that alcohols, diols, and hydrooxyketones reacting with N_2O_5 could produce organic nitrates: $R_1OH + N_2O_5 \rightarrow R_1ONO_2 + HNO_3$. We thus defined R_1OH and R_1ONO_2 as an oxidation-product pair, with an element difference of $-H+NO_2$. In addition, the organic nitrates are suggested to undergo hydrolysis, with the formation of HNO_3: $R_2ONO_2 + H_2O \rightarrow R_2OH + HNO_3$; R_2ONO_2 and R_2OH are defined as a hydrolyzation-product pair. Sometimes, $CHON_1$ can define as an oxidation-product pair with CHO and a hydrolyzation-product pair with $CHON_2$. If the two processes occur simultaneously, we defined this molecule as a potential mixed-processes product. A more detailed description of the three processes was presented elsewhere (Su et al., 2021).

Figures 4d, and 4e show potential pathways of CHON– molecules (CHON+ in Fig. S10) assigned to C1, C2, and C3, respectively. The result showed that oxidation-product pair, hydrolyzation-product pair, and mixed-processesproduct could explain a significant proportion, with 33 %–75 %, 69 %–77 %, and 44 %–80 % of CHON formulas assigned to C1, C2, and C3, respectively, which is comparable to the explained proportion of 52.8 %–69.7 % for $CHON_1$ and 43.4 %–53.5 % for $CHON_2$ in snow samples (Su et al., 2021). $CHON_1$ formulas assigned to C1 and C2 exhibited the highest proportion of oxidation from CHO, yet the primary precursor types are aliphatic compounds (52 %) and highly unsaturated and phenolic compounds (30 %) for C1 and highly unsaturated and phenolic compounds (54 %) and aromatic/condensed aromatic compounds (40 %) for C2, respectively (Figs. 4f, and 4g). Whereas $CHON_1$ assigned to C3 exhibited the highest proportion of mixed-processes product. Note that C1 and

https://doi.org/10.5194/egusphere-2023-403
Preprint. Discussion started: 29 March 2023

C3 formulas contain fewer $CHON_2$ and $CHON_3$ formulas, which is no longer to discuss them. Conversely, C2 formulas contain abundant $CHON_2$ and $CHON_3$ formulas, and the potential oxidation-product pairs from $CHON_1$ ($CHON_2$) contributed to 69 % of $CHON_2$ (77 % of $CHON_3$), largely deriving from highly unsaturated and phenolic compounds and aromatic compounds. In contrast to ESI–, the contribution determined by the three processes decreased with the portion of 5 %–73 %, 29 %–65 %, and 0–17 % for C1–3-assigned CHON+ formulas, respectively. Due to the small number of $CHON_{2-3}$ formulas assigned to C1 and $CHON_{1-3}$ formulas assigned to C3, we only discussed $CHON_1$ of C1 and $CHON_{1-3}$ of C2 (Fig. S10). The hydrolyzation process contributed 38 %, and oxidation-product pairs contributed 30 % of C1-assigned $CHON_1$. In contrast, oxidation-product pairs contributed to 29 %–48 % for C2-assigned $CHON_{1-3}$ formulas, yet the main precursor types are highly unsaturated and phenolic (56 %–70 %) and aliphatic compounds (20 %–33 %), different from C1 (Fig. S10g). Overall, although hydrolyzation-product pairs contributed to C1-assigned CHON+ formulas, the result showed that oxidation is one of the key formation pathways for the abundant CHON formulas assigned to HULIS components, especially C2. N-containing compounds, in particular CHON compounds, substantially contributed a lot of light absorption of BrC (Lin et al., 2017; Bluvshtein et al., 2017). The significant differences in the formation processes of CHON compounds assigned to PARAFAC components may be an important factor affecting the light absorption of BrC, even radiation forcing.

https://doi.org/10.5194/egusphere-2023-403
Preprint. Discussion started: 29 March 2023

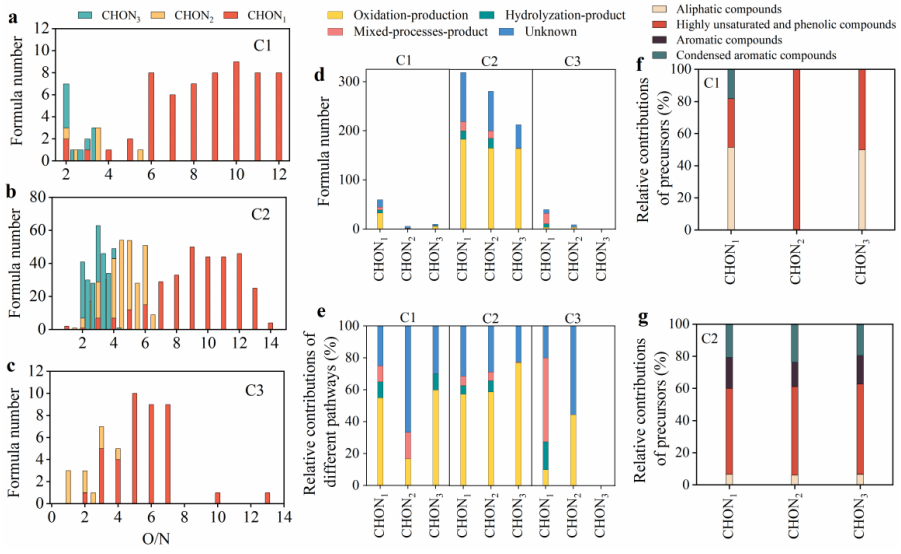

Figure 4. O/N ratios distribution of CHON– compounds assigned to C1 (a), C2 (b), and C3 (c), and the corresponding formula number distribution of different pathways for CHON– molecules assigned to C1–3 (d) and the relative contributions of different pathways (e). Indeed, panels (f–g) refer to the relative contributions of different precursor types to the abundant oxidation-product pair for $CHON_{1\text{-}3}$ of C1 and C2, respectively.

Multiple studies have demonstrated that S-containing compounds have little or no contribution to BrC chromophores (Song et al., 2019; Zeng et al., 2021), yet knowledge of the formation pathway of S-containing compounds assigned to PARAFAC components could help us understand its formation mechanism with possible similar pathways. Previous work investigated the prevalence of the epoxide formation pathway for organosulfates (OS) and nitrooxy-OS by examining the presence of precursor-product pairs of the CHOS (or CHONS) and the corresponding CHO (or CHON) compounds (Lin et al., 2012b). If the epoxides form, both sulfate and water can act as nucleophiles, and thus, both the OS and the corresponding alcohol should be present. In our samples, although few S-containing compounds were assigned to C1 (19, 20 % of its formulas) and C2 (56, 4.2 %) in that were less than C3 (117, 47 %), 84 %–100 % of CHOS compounds assigned to PARAFAC components had O/S ratios > 4, and 15 %–70 % of CHONS compounds had O/S > 7 for $CHON_1S$ compounds, and > 10 for $CHON_2S$ compounds, which satisfied the epoxides pathway. In Table 1, a similar

https://doi.org/10.5194/egusphere-2023-403
Preprint. Discussion started: 29 March 2023

480 analysis shows this process over CHOS and CHONS assigned to three PARAFAC
481 components. On average, for over 26 %–58 % of CHOS assigned to C1–3, the
482 corresponding CHO alcohol formulas were found, consistent with the epoxide
483 intermediate pathway for OS formation, yet the remaining 42 %–74 % of CHOS, have
484 no corresponding alcohols, may be formed from other pathways. In contrast, only a
485 small fraction of CHONS OS assigned to C1 and C2 were observed as exist for the
486 corresponding CHON alcohol formulas, yet this fraction increased to 47 % of CHONS
487 OS assigned to C3, implying that the epoxide pathway is more significant for the
488 formation of OS in the CHONS assigned to C3. In addition, previous work showed that
489 organonitrates hydrolyze more rapidly than OS (Hu et al., 2011). This hydrolysis
490 process could substitute the nitrooxy group with a hydroxyl group (i.e., $-HNO_3 + H_2O$).
491 On average for 76 % of CHOS assigned to C3 (Table 1), a corresponding CHONS is
492 present, which could be explained by the hydrolysis of nitrooxy groups of OS, yet not
493 common for CHOS assigned to C1 and C2. The prevalent hydrolysis of nitrooxy groups
494 of OS is commonly observed in the Pearl River Delta of China and Bakersfield,
495 California (Lin et al., 2012b; O'Brien et al., 2014). This collectively indicated that the
496 CHOS assigned to C3 mainly derived from the epoxide intermediate pathway and
497 hydrolysis process (80 %), and CHONS were mainly derived from the epoxide
498 intermediate pathway.

499 **Table 1**. Numbers and percentages of formation and hydrolysis reactions of CHOS and CHONS.

Number and Percentages of Precursor-Product Pairs				
Sample type	CHOS–SO_3→CHO	CHONS–SO_3→CHON	CHONS+OH–NO_3→CHOS	References
Karachi, Pakistan				
C1	11 (58 %)	2 (22 %)	0 (0.0 %)	This study
C2	12 (26 %)	0 (0.0 %)	2 (4.3 %)	
C3	26 (31 %)	16 (47 %)	63 (76 %)	
Bakersfield, California				(O'Brien et al., 2014)
Midnight to 6 A.M.	77 (45 %)	17 (30 %)	43 (74 %)	
6 A.M. to Noon	70 (41 %)	17 (27 %)	53 (79 %)	
Noon to 6 P.M.	115 (63 %)	12 (41 %)	26 (75 %)	
6 P.M. to Midnight	131 (79 %)	10 (30 %)	22 (66 %)	

https://doi.org/10.5194/egusphere-2023-403
Preprint. Discussion started: 29 March 2023

Guangzhou, China				
Urban	148 (65 %)	2 (2.8 %)	52 (75 %)	
Suburban	74 (69 %)	7 (15 %)	22 (47 %)	(Lin et al., 2012b)
Rural	113 (75 %)	3 (5.1 %)	38 (69 %)	
Urban	699 (27 %)	508 (19 %)	-	(Jiang et al., 2022a)

Numbers and percent of CHOS and CHONS compounds with corresponding CHO, CHON, and CHOS formulas in the same mass spectra for the following reactions: $C_xH_yO_zS \rightarrow C_xH_yO_{z-3} + SO_3$; $C_xH_yO_zN_wS \rightarrow C_xH_yO_{z-3}N_w + SO_3$; $C_xH_yO_zN_wS \rightarrow C_xH_{y+1}O_{z-2}N_{w-1}S - H_2O + HNO_3$.

The remaining O-containing compounds, including CHO–, CHO+, and CHONa+ groups, are mainly substituted with multiple polar functionalities including carboxyl, carbonyl, and hydroxyl groups. Except for the primary emission source for CHO compounds, secondary formation was suggested to occur (Lee et al., 2014; Lin et al., 2014). Kundu et al. (2012) detected hundreds of CHO molecules in SOA from limonene ozonolysis. Specially, 42 % of CHO compounds (neutral molecules) assigned to C1, 34 % assigned to C2, and 5.3 % assigned to C3 were commonly detected in mass spectra of limonene ozonolysis samples (Table S5), indicating a significant fraction of the oxidation process for the formation of CHO compounds assigned to C1 and C2. Undoubtedly, aging (e.g., NH_3) of limonene ozonolysis SOA is susceptible to the formation of oligomeric products with extensive conjugation of π-bonds creating the BrC chromophores (Laskin et al., 2014). In contrast, some CHO assigned to C2 was observed in the naphthalene photooxidation products, biomass burning, and aqueous-phase reactions of phenols (Table S6), yet not common for CHO assigned to C1 and C3. Remarkably, a majority of CHO (about 90 %) assigned to C3 may be formed from the other pathways. The n_c-OSc space of the CHO compounds assigned to C3 allowed for a probable hydrocarbon-like OA and biomass-burning OA source for this group (Fig. S11) (Kroll et al., 2011). Overall, the obtained formation pathways for PARAFAC components based on their molecular composition may explain the molecular similarity in C1 and C2 as described above. For example, 36 % of overlapped CHON compounds in C1 and C2 formulas were observed as oxidation-product pair, and 73 % of overlapped CHO compounds were detected in limonene ozonolysis SOA, suggesting that the

https://doi.org/10.5194/egusphere-2023-403
Preprint. Discussion started: 29 March 2023

oxidation reaction may be an important reason for their molecular-level correlation of C1 and C2.

3.4. Underlying implication of PARAFAC component to BrC absorption

The exact molecular identities of the BrC chromophores are expected to have a high degree of conjugation across the molecular skeleton and large absorption cross-sections (Lin et al., 2018). Fluorescence is a subset of BrC chromophores that absorb certain wavelengths of light and re-emit a fraction of that energy. Thus, the components decomposed by PARAFAC analysis represent a category of compounds that have similar chemical properties, which can define as the chemical identification of BrC chromophores. Our recent work found that the PARAFAC component with the longest-emission maxima had the largest coefficient by fitting the light absorption and PARAFAC components using multiple linear regression (Tang et al., 2021), indicating that this component could significantly contribute to light absorption. However, the molecular-level correlation between PARAFAC components and BrC chromophores was not fully understood. Solving this gap could promote the application of the EEM-PARAFAC method for studying BrC chromophores. Lin et al. (2018) proposed a plot of carbon number versus DBE based on the formulas, and the compounds with DBE/C ratios of 0.5~0.9 are potential BrC chromophores. The shaded area in Fig. 5 highlights the molecules assigned to C1–3 matching this criterion. Of the formulas assigned to C1, 37 % of ESI– and 16 % of ESI+ formulas are located in the “BrC domain” marked by the brown area. In contrast, a larger number of C2 formulas are located in this region, accounting for 65 % and 31 % of total C2 formulas detected in the ESI– and ESI+, respectively, yet only 12 % of ESI– and 21 % of ESI+ formulas assigned to C3 are within “BrC domain”. The result implied that a category of compounds that produce C2 fluorophores could substantially contribute to the light absorption of BrC, as further confirmed by the highly overlapped formulas between C2 and BrC-assigned formulas (72 %–94 % of C2 formulas and 47 %–57 % of BrC formulas) (Fig. S9). This may be

https://doi.org/10.5194/egusphere-2023-403
Preprint. Discussion started: 29 March 2023

the molecular basis for the tight correlation between C2 and MAE_{365} observed in this study. Undoubtedly, the NO_x addition reaction generally produced highly absorbing substances (Li et al., 2020a; He et al., 2022; Siemens et al., 2022), as this process largely occurred in the formation of C2, suggesting that the molecular consistency between C2 and BrC may be due to the NO_x addition reaction. Remarkably, some of the molecules assigned to PARAFAC components were observed as not matching this region, perhaps because they underwent similar processes like BrC chromophores. In general, the statistical significance of correlation provides more intrinsic information for understanding the molecular basis and fate of atmospheric PARAFAC components, even to BrC chromophores.

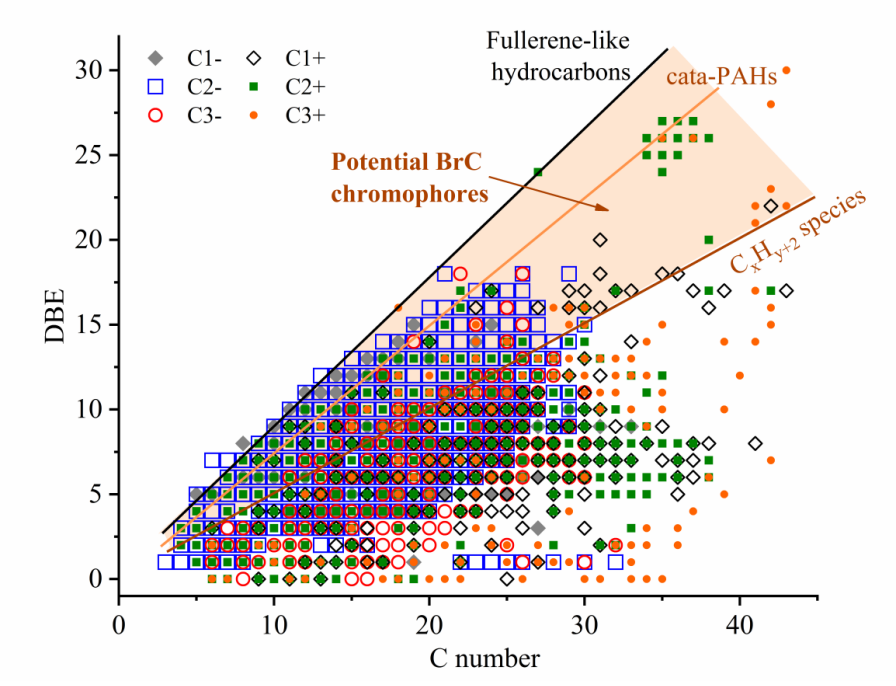

Figure 5. Plot of the double bond equivalent (DBE) vs the number of carbon atoms in PARAFAC components-assigned molecular formulas. Lines indicate DBE reference values of linear conjugated polyenes C_xH_{x+2} with DBE = 0.5 × c (brown solid line), *cata*-condensed PAHs (yellow solid line), and fullerene-like hydrocarbons with DBE = 0.9 × c (black solid line). Data points inside the orange-shaded area are potential BrC chromophores (Lin et al., 2018).

https://doi.org/10.5194/egusphere-2023-403
Preprint. Discussion started: 29 March 2023

4. Conclusions and atmospheric implications

In this study, the fluorescence and molecular compositions of water extracts in Karachi aerosol were characterized using EEM spectroscopy and negative and positive ESI FT-ICR MS, respectively. The identified two humic-like (C1 and C2) and one protein-like (C3) components are commonly observed in the atmosphere, which has different molecular characteristics and formation pathways. The characteristics of fluorescent components may be indicative of the sources, atmospheric processes, and reactivity of water-soluble aerosol components. Of what we observed in this study, C1 and C2 were enriched in N-containing compounds, yet C2 is more associated with higher aromaticity, higher N content, and highly oxygenated compounds; C3 is characterized as low conjugation, oxygen-depleted, N-depleted, but S-enriched species. Previous studies showed that fluorescent components may be employed as source indicators for OA (Chen et al., 2016b; Tang et al., 2020). Aromatic compounds generally originate from combustion emissions; fluorescent components with high aromatic moieties, such as the C2 component, may be derived from anthropogenic precursors that have experienced high oxidation (high NOSC and $\overline{OS}_C$). However, the feature of C3 may originate from primary emissions, e.g., vehicular exhaust (Mladenov et al., 2011).

Oxidation formation pathway was observed as an important process for the formation of C1 and C2, especially their assigned CHON compounds. The O/C ratios of C1- and C2-assigned ESI– compounds (0.48±0.18 and 0.59±0.20, respectively) also exhibit higher values, especially C2, than that from primary emissions and some SOA, as shown in Fig. 6. This molecular-level character of C2 indicates that this component may be used as a secondary source tracer, consistent with a recent study observed using online EEM monitoring (Chen et al., 2021b). The secondary information involved could be used to probe the secondary source of BrC, which is poorly understood because of its chemical complexity. In addition, C2 with the longest emission maxima (~494 nm), was assigned to a large number of compounds that matched the “potential BrC” region

https://doi.org/10.5194/egusphere-2023-403
Preprint. Discussion started: 29 March 2023

and overlapped with BrC-associated formulas, and readily correlated tightly with MAE_{365}, collectively indicating that a category of compounds illuminating C2 may significantly contribute to the BrC light absorption, which also observed in our previous study (Tang et al., 2021). In the study of Chen et al. (2019), they showed that almost all DTT activity is attributed to the C7 chromophore (99%), a component similar to C2 in this study. Given the high light absorption radiation and health effect induced by C2, much attention should be drawn to further study. It is also suggested that the commonly used fluorescence characteristics derived from aquatic environments may not be applicable, as references, to atmospheric WSOC study (refer to Text S7). Our findings on the molecular compositions and formation mechanisms of atmospheric fluorescent components are expected to be helpful to further studies using the EEM-PARAFAC as a tool to study atmospheric BrC (Laskin et al., 2015).

https://doi.org/10.5194/egusphere-2023-403
Preprint. Discussion started: 29 March 2023

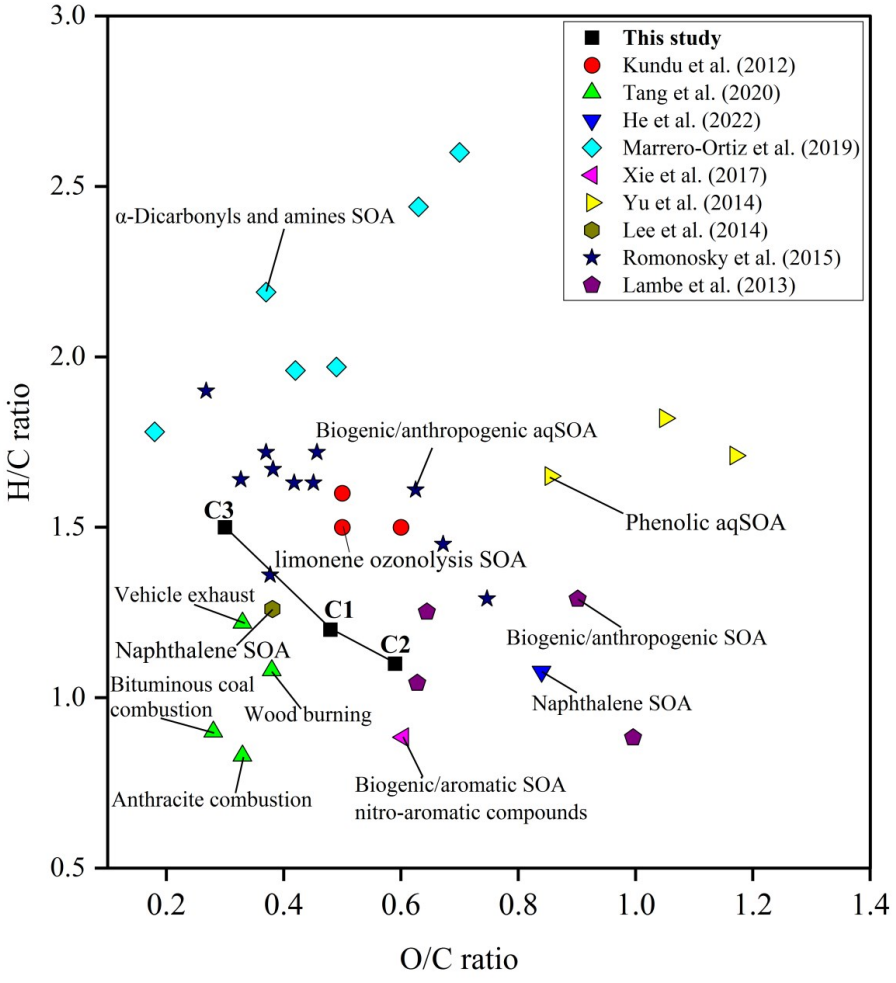

Figure 6. Comparison of O/C and H/C ratios of C1–3 assigned ESI– compounds in water-soluble organic compounds in this study with other primary emissions and secondary organic aerosol.

https://doi.org/10.5194/egusphere-2023-403
Preprint. Discussion started: 29 March 2023

Data availability. The data used in this study are available in the Harvard Dataverse (https://doi.org/10.7910/DVN/RWIJZT, Tang, 2023).

Supplement. The supplement related to this article is available online.

Author Contributions. GaZ and JT designed the study. JH provided the samples. JT, YM, HJ, ZZ, and BJ carried out the analysis. JianT provided the instrument. JT processed the data and wrote the original draft. JL, SZ, GuZ, YC, CT, JS, and GaZ review the manuscript.

Competing interests. The authors declare that they have no conflict of interest.

Acknowledgments. We appreciate Boji and Yangzhi for their help with the model and FT-ICR MS analysis.

Financial support. This research has been supported by the National Natural Science Foundation of China (Grant nos. 42030715 and 42207308), the Alliance of International Science Organizations (ANSO-CR-KP-2021-05), the Guangdong Basic and Applied Basic Research Foundation (2017BT01Z134, 2021A0505020017, and 2023B1515020067), and Youth Innovation Promotion Association, CAS (2022359).

References:

Bianco, A., Minella, M., De Laurentiis, E., Maurino, V., Minero, C., and Vione, D.: Photochemical generation of photoactive compounds with fulvic-like and humic-like fluorescence in aqueous solution, Chemosphere, 111, 529-536, https://doi.org/10.1016/j.chemosphere.2014.04.035, 2014.

Bluvshtein, N., Lin, P., Flores, J. M., Segev, L., Mazar, Y., Tas, E., Snider, G., Weagle, C., Brown, S. S., Laskin, A., and Rudich, Y.: Broadband optical properties of biomass-burning aerosol and identification of brown carbon chromophores, J. Geophys. Res.-Atmos., 122, 5441-5456, https://doi.org/10.1002/2016jd026230, 2017.

Bosch, C., Andersson, A., Kirillova, E. N., Budhavant, K., Tiwari, S., Praveen, P. S., Russell, L. M., Beres, N. D., Ramanathan, V., and Gustafsson, Ö.: Source-diagnostic dual-isotope composition and optical properties of water-soluble organic carbon and elemental carbon in the South Asian outflow intercepted over the Indian Ocean, J. Geophys. Res.-Atmos., 119, 11,743-711,759, https://doi.org/10.1002/2014jd022127, 2014.

https://doi.org/10.5194/egusphere-2023-403
Preprint. Discussion started: 29 March 2023

Chen, P., Kang, S., Tripathee, L., Ram, K., Rupakheti, M., Panday, A. K., Zhang, Q., Guo, J., Wang, X., Pu, T., and Li, C.: Light absorption properties of elemental carbon (EC) and water-soluble brown carbon (WS-BrC) in the Kathmandu Valley, Nepal: A 5-year study, Environ. Pollut., 261, 114239, https://doi.org/10.1016/j.envpol.2020.114239, 2020.

Chen, Q., Ikemori, F., Higo, H., Asakawa, D., and Mochida, M.: Chemical Structural Characteristics of HULIS and Other Fractionated Organic Matter in Urban Aerosols: Results from Mass Spectral and FT-IR Analysis, Environ. Sci. Technol., 50, 1721-1730, https://doi.org/10.1021/acs.est.5b05277, 2016a.

Chen, Q., Miyazaki, Y., Kawamura, K., Matsumoto, K., Coburn, S., Volkamer, R., Iwamoto, Y., Kagami, S., Deng, Y., Ogawa, S., Ramasamy, S., Kato, S., Ida, A., Kajii, Y., and Mochida, M.: Characterization of Chromophoric Water-Soluble Organic Matter in Urban, Forest, and Marine Aerosols by HR-ToF-AMS Analysis and Excitation-Emission Matrix Spectroscopy, Environ. Sci. Technol., 50, 10351-10360, https://doi.org/10.1021/acs.est.6b01643, 2016b.

Chen, Q., Wang, M., Wang, Y., Zhang, L., Li, Y., and Han, Y.: Oxidative Potential of Water-Soluble Matter Associated with Chromophoric Substances in $PM_{2.5}$ over Xi'an, China, Environ. Sci. Technol., 53, 8574-8584, https:// doi.org/10.1021/acs.est.9b01976, 2019.

Chen, Q., Hua, X., and Dyussenova, A.: Evolution of the chromophore aerosols and its driving factors in summertime Xi'an, Northwest China, Chemosphere, 281, 130838, https://doi.org/10.1016/j.chemosphere.2021.130838, 2021a.

Chen, Q., Hua, X., Li, J., Chang, T., and Wang, Y.: Diurnal evolutions and sources of water-soluble chromophoric aerosols over Xi'an during haze event, in Northwest China, Sci. Total Environ., 786, 147412, https://doi.org/10.1016/j.scitotenv.2021.147412, 2021b.

Choudhary, V., Rajput, P., Singh, D. K., Singh, A. K., and Gupta, T.: Light absorption characteristics of brown carbon during foggy and non-foggy episodes over the Indo-Gangetic Plain, Atmos. Pollut. Res., 9, 494-501, https://doi.org/10.1016/j.apr.2017.11.012, 2018.

Choudhary, V., Rajput, P., and Gupta, T.: Absorption properties and forcing efficiency of light-absorbing water-soluble organic aerosols: Seasonal and spatial variability, Environ. Pollut., 272, 115932, https://doi.org/10.1016/j.envpol.2020.115932, 2021.

Choudhary, V., Gupta, T., and Zhao, R.: Evolution of Brown Carbon Aerosols during Atmospheric Long-Range Transport in the South Asian Outflow and Himalayan Cryosphere, ACS Earth and Space Chemistry, 6, 2335-2347, https://doi.org/10.1021/acsearthspacechem.2c00047, 2022.

Coble, P. G.: Marine optical biogeochemistry: The chemistry of ocean color, Chem. Rev., 107, 402-418, https://doi.org/10.1021/cr050350, 2007.

Dasari, S., Andersson, A., Bikkina, S., Holmstrand, H., Budhavant, K., Satheesh, S. K., Asmi, E., Kesti, J., Backman, J., and Salam, A.: Photochemical degradation affects the light absorption of water-soluble brown carbon in the South Asian outflow, Sci. Adv., 5, https://doi.org/10.1126/sciadv.aau8066, 2019.

Fan, X. J., Cao, T., Yu, X. F., Wang, Y., Xiao, X., Li, F. Y., Xie, Y., Ji, W. C., Song, J. Z., and Peng, P. A.: The evolutionary behavior of chromophoric brown carbon during ozone aging of fine particles from biomass burning, Atmos. Chem. Phys., 20, 4593-4605, https://doi.org/10.5194/acp-20-4593-2020, 2020.

https://doi.org/10.5194/egusphere-2023-403
Preprint. Discussion started: 29 March 2023

Feng, Y., Ramanathan, V., and Kotamarthi, V. R.: Brown carbon: a significant atmospheric absorber of solar radiation?, Atmos. Chem. Phys., 13, 8607-8621, https://doi.org/10.5194/acp-13-8607-2013, 2013.

Gilardoni, S., Massoli, P., Paglione, M., Giulianelli, L., Carbone, C., Rinaldi, M., Decesari, S., Sandrini, S., Costabile, F., Gobbi, G. P., Pietrogrande, M. C., Visentin, M., Scotto, F., Fuzzi, S., and Facchini, M. C.: Direct observation of aqueous secondary organic aerosol from biomass-burning emissions, Proc Natl Acad Sci U S A, 113, 10013-10018, https://doi.org/10.1073/pnas.1602212113, 2016.

Han, H., Kim, G., Seo, H., Shin, K.-H., and Lee, D.-H.: Significant seasonal changes in optical properties of brown carbon in the midlatitude atmosphere, Atmos. Chem. Phys., 20, 2709-2718, https://doi.org/10.5194/acp-20-2709-2020, 2020.

He, Q., Li, C., Siemens, K., Morales, A. C., Hettiyadura, A. P. S., Laskin, A., and Rudich, Y.: Optical Properties of Secondary Organic Aerosol Produced by Photooxidation of Naphthalene under NOx Condition, Environ. Sci. Technol., 56, 4816-4827, https://doi.org/10.1021/acs.est.1c07328, 2022.

Hecobian, A., Zhang, X., Zheng, M., Frank, N., Edgerton, E. S., and Weber, R. J.: Water-Soluble Organic Aerosol material and the light-absorption characteristics of aqueous extracts measured over the Southeastern United States, Atmos. Chem. Phys., 10, 5965-5977, https://doi.org/10.5194/acp-10-5965-2010, 2010.

Hernes, P. J., Bergamaschi, B. A., Eckard, R. S., and Spencer, R. G. M.: Fluorescence-based proxies for lignin in freshwater dissolved organic matter, J. Geophys. Res.: Biogeosciences, 114, https://doi.org/10.1029/2009JG000938, 2009.

Hertkorn, N., Benner, R., Frommberger, M., Schmitt-Kopplin, P., Witt, M., Kaiser, K., Kettrup, A., and Hedges, J. I.: Characterization of a major refractory component of marine dissolved organic matter, Geochim. Cosmochim. Acta, 70, 2990-3010, https://doi.org/10.1016/j.gca.2006.03.021, 2006.

Hu, K. S., Darer, A. I., and Elrod, M. J.: Thermodynamics and kinetics of the hydrolysis of atmospherically relevant organonitrates and organosulfates, Atmos. Chem. Phys., 11, 8307-8320, https://doi.org/10.5194/acp-11-8307-2011, 2011.

Ishii, S. K., and Boyer, T. H.: Behavior of reoccurring PARAFAC components in fluorescent dissolved organic matter in natural and engineered systems: a critical review, Environ. Sci. Technol., 46, 2006-2017, https://doi.org/10.1021/es2043504, 2012.

Jiang, B., Liang, Y., Xu, C., Zhang, J., Hu, M., and Shi, Q.: Polycyclic Aromatic Hydrocarbons (PAHs) in Ambient Aerosols from Beijing: Characterization of Low Volatile PAHs by Positive-Ion Atmospheric Pressure Photoionization (APPI) Coupled with Fourier Transform Ion Cyclotron Resonance, Environ. Sci. Technol., 48, 4716-4723, https://doi.org/10.1021/es405295p, 2014.

Jiang, H., Li, J., Sun, R., Tian, C., Tang, J., Jiang, B., Liao, Y., Chen, C.-E., and Zhang, G.: Molecular Dynamics and Light Absorption Properties of Atmospheric Dissolved Organic Matter, Environ. Sci. Technol., 55, 10268-10279, https://doi.org/10.1021/acs.est.1c01770, 2021.

Jiang, H., Li, J., Tang, J., Cui, M., Zhao, S., Mo, Y., Tian, C., Zhang, X., Jiang, B., Liao, Y., Chen, Y., and Zhang, G.: Molecular characteristics, sources, and formation pathways of organosulfur

https://doi.org/10.5194/egusphere-2023-403
Preprint. Discussion started: 29 March 2023

compounds in ambient aerosol in Guangzhou, South China, Atmos. Chem. Phys., 22, 6919-6935, https://doi.org/10.5194/acp-22-6919-2022, 2022a.

Jiang, H., Li, J., Tang, J., Zhao, S., Chen, Y., Tian, C., Zhang, X., Jiang, B., Liao, Y., and Zhang, G.: Factors Influencing the Molecular Compositions and Distributions of Atmospheric Nitrogen‐Containing Compounds, J. Geophys. Res.-Atmos., 127, https://doi.org/10.1029/2021jd036284, 2022b.

Jiang, H., Tang, J., Li, J., Zhao, S., Mo, Y., Tian, C., Zhang, X., Jiang, B., Liao, Y., Chen, Y., and Zhang, G.: Molecular Signatures and Sources of Fluorescent Components in Atmospheric Organic Matter in South China, Environ. Sci. Technol. Lett., 9, 913-920, https://doi.org/10.1021/acs.estlett.2c00629, 2022c.

Kames, J., Schurath, U., Flocke, F., and Volz-Thomas, A.: Preparation of organic nitrates from alcohols and N_2O_5 for species identification in atmospheric samples, J. Atmos. Chem., 16, 349-359, https://doi.org/10.1007/BF01032630, 1993.

Kellerman, A. M., Kothawala, D. N., Dittmar, T., and Tranvik, L. J.: Persistence of dissolved organic matter in lakes related to its molecular characteristics, Nat. Geosci., 8, 454-U452, https://doi.org/10.1038/ngeo2440, 2015.

Khwaja, H. A., Parekh, P. P., Khan, A. R., Hershey, D. L., Naqvi, R. R., Malik, A., and Khan, K.: An In-Depth Characterization of Urban Aerosols Using Electron Microscopy and Energy Dispersive X-Ray Analysis, CLEAN – Soil, Air, Water, 37, 544-554, https://doi.org/10.1002/clen.200900012, 2009.

Kirchstetter, T. W., and Thatcher, T. L.: Contribution of organic carbon to wood smoke particulate matter absorption of solar radiation, Atmos. Chem. Phys., 12, 5803-5816, https://doi.org/10.5194/acp-12-6067-2012, 2012.

Kirillova, E. N., Andersson, A., Tiwari, S., Srivastava, A. K., Bisht, D. S., and Gustafsson, Ö.: Water-soluble organic carbon aerosols during a full New Delhi winter: Isotope-based source apportionment and optical properties, J. Geophys. Res.-Atmos., 119, 3476-3485, https://doi.org/10.1002/2013jd020041, 2014.

Kroll, J. H., Donahue, N. M., Jimenez, J. L., Kessler, S. H., Canagaratna, M. R., Wilson, K. R., Altieri, K. E., Mazzoleni, L. R., Wozniak, A. S., Bluhm, H., Mysak, E. R., Smith, J. D., Kolb, C. E., and Worsnop, D. R.: Carbon oxidation state as a metric for describing the chemistry of atmospheric organic aerosol, Nat. Chem., 3, 133-139, https://doi.org/10.1038/nchem.948, 2011.

Kundu, S., Fisseha, R., Putman, A. L., Rahn, T. A., and Mazzoleni, L. R.: High molecular weight SOA formation during limonene ozonolysis: insights from ultrahigh-resolution FT-ICR mass spectrometry characterization, Atmos. Chem. Phys., 12, 5523-5536, https://doi.org/10.5194/acp-12-5523-2012, 2012.

Lambe, A. T., Cappa, C. D., Massoli, P., Onasch, T. B., Forestieri, S. D., Martin, A. T., Cummings, M. J., Croasdale, D. R., Brune, W. H., Worsnop, D. R., and Davidovits, P.: Relationship between oxidation level and optical properties of secondary organic aerosol, Environ. Sci. Technol., 47, 6349-6357, https://doi.org/10.1021/es401043j, 2013.

Lamkaddam, H., Dommen, J., Ranjithkumar, A., Gordon, H., Wehrle, G., Krechmer, J., Majluf, F., Salionov, D., Schmale, J., Bjelic, S., Carslaw, K. S., El Haddad, I., and Baltensperger, U.: Large

https://doi.org/10.5194/egusphere-2023-403
Preprint. Discussion started: 29 March 2023

contribution to secondary organic aerosol from isoprene cloud chemistry, Sci. Adv., 7, https://doi.org/10.1126/sciadv.abe2952, 2021.

Laskin, A., Laskin, J., and Nizkorodov, S. A.: Chemistry of atmospheric brown carbon, Chem. rev., 115, 4335-4382, https://doi.org/10.1021/cr5006167, 2015.

Laskin, J., Laskin, A., Nizkorodov, S. A., Roach, P., Eckert, P., Gilles, M. K., Wang, B., Lee, H. J., and Hu, Q.: Molecular selectivity of brown carbon chromophores, Environ. Sci. Technol., 48, 12047-12055, https://doi.org/10.1021/es503432r, 2014.

Lee, H. J., Laskin, A., Laskin, J., and Nizkorodov, S. A.: Excitation-emission spectra and fluorescence quantum yields for fresh and aged biogenic secondary organic aerosols, Environ. Sci. Technol., 47, 5763-5770, https://doi.org/10.1021/es400644c, 2013.

Lee, H. J., Aiona, P. K., Laskin, A., Laskin, J., and Nizkorodov, S. A.: Effect of solar radiation on the optical properties and molecular composition of laboratory proxies of atmospheric brown carbon, Environ. Sci. Technol., 48, 10217-10226, https://doi.org/10.1021/es502515r, 2014.

Li, C., He, Q., Fang, Z., Brown, S. S., Laskin, A., Cohen, S. R., and Rudich, Y.: Laboratory Insights into the Diel Cycle of Optical and Chemical Transformations of Biomass Burning Brown Carbon Aerosols, Environ. Sci. Technol., 54, 11827-11837, https://doi.org/10.1021/acs.est.0c04310, 2020a.

Li, J., Zhang, Q., Wang, G., Li, J., Wu, C., Liu, L., Wang, J., Jiang, W., Li, L., Ho, K. F., and Cao, J.: Optical properties and molecular compositions of water-soluble and water-insoluble brown carbon (BrC) aerosols in northwest China, Atmos. Chem. Phys., 20, 4889-4904, https://doi.org/10.5194/acp-20-4889-2020, 2020b.

Li, M., Fan, X., Zhu, M., Zou, C., Song, J., Wei, S., Jia, W., and Peng, P.: Abundances and light absorption properties of brown carbon emitted from residential coal combustion in China, Environ. Sci. Technol., 53, 595-603, https://doi.org/10.1021/acs.est.8b05630, 2018.

Li, S., Fan, R., Luo, D., Xue, Q., Li, L., Yu, X., Huang, T., Yang, H., and Huang, C.: Variation in quantity and quality of rainwater dissolved organic matter (DOM) in a peri-urban region: Implications for the effect of seasonal patterns on DOM fates, Atmos. Environ., 239, 117769, https://doi.org/10.1016/j.atmosenv.2020.117769, 2020c.

Li, X., Yu, F., Cao, J., Fu, P., Hua, X., Chen, Q., Li, J., Guan, D., Tripathee, L., Chen, Q., and Wang, Y.: Chromophoric dissolved organic carbon cycle and its molecular compositions and optical properties in precipitation in the Guanzhong basin, China, Sci. Total Environ., 152775, https://doi.org/10.1016/j.scitotenv.2021.152775, 2022.

Lin, P., Huang, X.-F., He, L.-Y., and Zhen Yu, J.: Abundance and size distribution of HULIS in ambient aerosols at a rural site in South China, J. Aerosol Sci, 41, 74-87, https://doi.org/10.1016/j.jaerosci.2009.09.001, 2010.

Lin, P., and Yu, J. Z.: Generation of reactive oxygen species mediated by humic-like substances in atmospheric aerosols, Environ. Sci. Technol., 45, 10362-10368, https://doi.org/10.1021/es2028229, 2011.

Lin, P., Rincon, A. G., Kalberer, M., and Yu, J. Z.: Elemental composition of HULIS in the Pearl River Delta Region, China: results inferred from positive and negative electrospray high resolution mass spectrometric data, Environ. Sci. Technol., 46, 7454-7462, https://doi.org/10.1021/es300285d, 2012a.

https://doi.org/10.5194/egusphere-2023-403
Preprint. Discussion started: 29 March 2023

Lin, P., Yu, J. Z., Engling, G., and Kalberer, M.: Organosulfates in humic-like substance fraction isolated from aerosols at seven locations in East Asia: a study by ultra-high-resolution mass spectrometry, Environ. Sci. Technol., 46, 13118-13127, https://doi.org/10.1021/es303570v, 2012b.

Lin, P., Bluvshtein, N., Rudich, Y., Nizkorodov, S. A., Laskin, J., and Laskin, A.: Molecular Chemistry of Atmospheric Brown Carbon Inferred from a Nationwide Biomass Burning Event, Environ. Sci. Technol., 51, 11561-11570, https://doi.org/10.1021/acs.est.7b02276, 2017.

Lin, P., Fleming, L. T., Nizkorodov, S. A., Laskin, J., and Laskin, A.: Comprehensive Molecular Characterization of Atmospheric Brown Carbon by High Resolution Mass Spectrometry with Electrospray and Atmospheric Pressure Photoionization, Anal. Chem., 90, 12493-12502, https://doi.org/10.1021/acs.analchem.8b02177, 2018.

Lin, Y. H., Budisulistiorini, S. H., Chu, K., Siejack, R. A., Zhang, H., Riva, M., Zhang, Z., Gold, A., Kautzman, K. E., and Surratt, J. D.: Light-absorbing oligomer formation in secondary organic aerosol from reactive uptake of isoprene epoxydiols, Environ. Sci. Technol., 48, 12012-12021, https://doi.org/10.1021/es503142b, 2014.

Maie, N., Scully, N. M., Pisani, O., and Jaffé, R.: Composition of a protein-like fluorophore of dissolved organic matter in coastal wetland and estuarine ecosystems, Water Res., 41, 563-570, https://doi.org/10.1016/j.watres.2006.11.006, 2007.

Marrero-Ortiz, W., Hu, M., Du, Z., Ji, Y., Wang, Y., Guo, S., Lin, Y., Gomez-Hermandez, M., Peng, J., Li, Y., Secrest, J., Levy Zamora, M., Wang, Y., An, T., and Zhang, R.: Formation and optical properties of brown carbon from small alpha-dicarbonyls and amines, Environ. Sci. Technol., 53, 117-126, https://doi.org/10.1021/acs.est.8b03995, 2019.

Mladenov, N., Alados-Arboledas, L., Olmo, F. J., Lyamani, H., Delgado, A., Molina, A., and Reche, I.: Applications of optical spectroscopy and stable isotope analyses to organic aerosol source discrimination in an urban area, Atmos. Environ., 45, 1960-1969, https://doi.org/10.1016/j.atmosenv.2011.01.029, 2011.

Mo, Y., Li, J., Jiang, B., Su, T., Geng, X., Liu, J., Jiang, H., Shen, C., Ding, P., Zhong, G., Cheng, Z., Liao, Y., Tian, C., Chen, Y., and Zhang, G.: Sources, compositions, and optical properties of humic-like substances in Beijing during the 2014 APEC summit: Results from dual carbon isotope and Fourier-transform ion cyclotron resonance mass spectrometry analyses, Environ. Pollut., 239, 322-331, https://doi.org/10.1016/j.envpol.2018.04.041, 2018.

Mo, Y., Zhong, G., Li, J., Liu, X., Jiang, H., Tang, J., Jiang, B., Liao, Y., Cheng, Z., and Zhang, G.: The Sources, Molecular Compositions, and Light Absorption Properties of Water‐Soluble Organic Carbon in Marine Aerosols From South China Sea to the Eastern Indian Ocean, J. Geophys. Res.-Atmos., 127, https://doi.org/10.1029/2021jd036168, 2022.

Mopper, K., Stubbins, A., Ritchie, J. D., Bialk, H. M., and Hatcher, P. G.: Advanced instrumental approaches for characterization of marine dissolved organic matter: Extraction techniques, mass spectrometry, and nuclear magnetic resonance spectroscopy, Chem. Rev., 107, 419-442, https://doi.org/10.1021/cr050359b, 2007.

Murphy, K. R., Stedmon, C. A., Graeber, D., and Bro, R.: Fluorescence spectroscopy and multi-way techniques. PARAFAC, Anal. Methods, 5, 6557-6566, https://doi.org/10.1039/c3ay41160e, 2013.

https://doi.org/10.5194/egusphere-2023-403
Preprint. Discussion started: 29 March 2023

O'Brien, R. E., Nguyen, T. B., Laskin, A., Laskin, J., Hayes, P. L., Liu, S., Jimenez, J. L., Russell, L. M., Nizkorodov, S. A., and Goldstein, A. H.: Probing molecular associations of field-collected and laboratory-generated SOA with nano-DESI high-resolution mass spectrometry, J. Geophys. Res.-Atmos., https://doi.org/118, 1042-1051, 10.1002/jgrd.50119, 2013.

O'Brien, R. E., Laskin, A., Laskin, J., Rubitschun, C. L., Surratt, J. D., and Goldstein, A. H.: Molecular characterization of S- and N-containing organic constituents in ambient aerosols by negative ion mode high-resolution Nanospray Desorption Electrospray Ionization Mass Spectrometry: CalNex 2010 field study, J. Geophys. Res.-Atmos., 119, 12,706-712,720, https://doi.org/10.1002/2014jd021955, 2014.

Park, S. S., and Yu, J.: Chemical and light absorption properties of humic-like substances from biomass burning emissions under controlled combustion experiments, Atmos. Environ., 136, 114-122, https://doi.org/10.1016/j.atmosenv.2016.04.022, 2016.

Romonosky, D. E., Laskin, A., Laskin, J., and Nizkorodov, S. A.: High-resolution mass spectrometry and molecular characterization of aqueous photochemistry products of common types of secondary organic aerosols, J. Phys. Chem. A, 119, 2594-2606, https://doi.org/10.1021/jp509476r, 2015.

She, Z., Wang, J., He, C., Pan, X., Li, Y., Zhang, S., Shi, Q., and Yue, Z.: The Stratified Distribution of Dissolved Organic Matter in an AMD Lake Revealed by Multi-sample Evaluation Procedure, Environ. Sci. Technol., 55, 8401-8409, https://doi.org/10.1021/acs.est.0c05319, 2021.

Siemens, K., Morales, A., He, Q., Li, C., Hettiyadura, A. P. S., Rudich, Y., and Laskin, A.: Molecular Analysis of Secondary Brown Carbon Produced from the Photooxidation of Naphthalene, Environ. Sci. Technol., 56, 3340-3353, https://doi.org/10.1021/acs.est.1c03135, 2022.

Singer, G. A., Fasching, C., Wilhelm, L., Niggemann, J., Steier, P., Dittmar, T., and Battin, T. J.: Biogeochemically diverse organic matter in Alpine glaciers and its downstream fate, Nat. Geosci., 5, 710-714, https://doi.org/10.1038/ngeo1581, 2012.

Song, J. Z., Li, M. J., Fan, X. J., Zou, C. L., Zhu, M. B., Jiang, B., Yu, Z. Q., Jia, W. L., Liao, Y. H., and Peng, P. A.: Molecular Characterization of Water- and Methanol-Soluble Organic Compounds Emitted from Residential Coal Combustion Using Ultrahigh-Resolution Electrospray Ionization Fourier Transform Ion Cyclotron Resonance Mass Spectrometry, Environ. Sci. Technol., 53, 13607-13617, https://doi.org/10.1021/acs.est.9b04331, 2019.

Srinivas, B., and Sarin, M. M.: Light absorbing organic aerosols (brown carbon) over the tropical Indian Ocean: impact of biomass burning emissions, Environ. Res. Lett., 8, 044042, https://doi.org/10.1088/1748-9326/8/4/044042, 2013.

Srinivas, B., and Sarin, M. M.: Brown carbon in atmospheric outflow from the Indo-Gangetic Plain: Mass absorption efficiency and temporal variability, Atmos. Environ., 89, 835-843, https://doi.org/10.1016/j.atmosenv.2014.03.030, 2014.

Srinivas, B., Rastogi, N., Sarin, M. M., Singh, A., and Singh, D.: Mass absorption efficiency of light absorbing organic aerosols from source region of paddy-residue burning emissions in the Indo-Gangetic Plain, Atmos. Environ., 125, 360-370, https://doi.org/10.1016/j.atmosenv.2015.07.017, 2016.

https://doi.org/10.5194/egusphere-2023-403
Preprint. Discussion started: 29 March 2023

Stubbins, A., Lapierre, J. F., Berggren, M., Prairie, Y. T., Dittmar, T., and del Giorgio, P. A.: What's in an EEM? Molecular signatures associated with dissolved organic fluorescence in boreal Canada, Environ. Sci. Technol., 48, 10598-10606, https://doi.org/10.1021/es502086e, 2014.

Su, S., Xie, Q., Lang, Y., Cao, D., Xu, Y., Chen, J., Chen, S., Hu, W., Qi, Y., Pan, X., Sun, Y., Wang, Z., Liu, C. Q., Jiang, G., and Fu, P.: High Molecular Diversity of Organic Nitrogen in Urban Snow in North China, Environ. Sci. Technol., 55, 4344-4356, https://doi.org/10.1021/acs.est.0c06851, 2021.

Sullivan, A. P., Pokhrel, R. P., Shen, Y., Murphy, S. M., Toohey, D. W., Campos, T., Lindaas, J., Fischer, E. V., and Collett Jr, J. L.: Examination of brown carbon absorption from wildfires in the western US during the WE-CAN study, Atmos. Chem. Phys., 22, 13389-13406, https://doi.org/10.5194/acp-22-13389-2022, 2022.

Tang, J., Li, J., Su, T., Han, Y., Mo, Y., Jiang, H., Cui, M., Jiang, B., Chen, Y., Tang, J., Song, J., Peng, P., and Zhang, G.: Molecular compositions and optical properties of dissolved brown carbon in biomass burning, coal combustion, and vehicle emission aerosols illuminated by excitation–emission matrix spectroscopy and Fourier transform ion cyclotron resonance mass spectrometry analysis, Atmos. Chem. Phys., 20, 2513-2532, https://doi.org/10.5194/acp-20-2513-2020, 2020.

Tang, J., Wang, J., Zhong, G., Jiang, H., Mo, Y., Zhang, B., Geng, X., Chen, Y., Tang, J., Tian, C., Bualert, S., Li, J., and Zhang, G.: Measurement report: Long-emission-wavelength chromophores dominate the light absorption of brown carbon in aerosols over Bangkok: impact from biomass burning, Atmos. Chem. Phys., 21, 11337-11352, https://doi.org/10.5194/acp-21-11337-2021, 2021.

Updyke, K. M., Nguyen, T. B., and Nizkorodov, S. A.: Formation of brown carbon via reactions of ammonia with secondary organic aerosols from biogenic and anthropogenic precursors, Atmos. Environ., 63, 22-31, https://doi.org/10.1016/j.atmosenv.2012.09.012, 2012.

Varga, B., Kiss, G., Ganszky, I., Gelencsér, A., and Krivácsy, Z.: Isolation of water-soluble organic matter from atmospheric aerosol, Talanta, 55, 561-572, https://doi.org/10.1016/S0039-9140(01)00446-5, 2001.

Vione, D., Albinet, A., Barsotti, F., Mekic, M., Jiang, B., Minero, C., Brigante, M., and Gligorovski, S.: Formation of substances with humic-like fluorescence properties, upon photoinduced oligomerization of typical phenolic compounds emitted by biomass burning, Atmos. Environ., 206, 197-207, https://doi.org/10.1016/j.atmosenv.2019.03.005, 2019.

Wang, H., Zhang, L., Huo, T., Wang, B., Yang, F., Chen, Y., Tian, M., Qiao, B., and Peng, C.: Application of parallel factor analysis model to decompose excitation-emission matrix fluorescence spectra for characterizing sources of water-soluble brown carbon in PM2.5, Atmos. Environ., 223, 117192, https://doi.org/10.1016/j.atmosenv.2019.117192, 2020a.

Wang, J., Jiang, H., Jiang, H., Mo, Y., Geng, X., Li, J., Mao, S., Bualert, S., Ma, S., Li, J., and Zhang, G.: Source apportionment of water-soluble oxidative potential in ambient total suspended particulate from Bangkok: Biomass burning versus fossil fuel combustion, Atmos. Environ., 235, 117624, https://doi.org/10.1016/j.atmosenv.2020.117624, 2020b.

Weishaar, J. L., Aiken, G. R., Bergamaschi, B. A., Fram, M. S., Fujii, R., and Mopper, K.: Evaluation of Specific Ultraviolet Absorbance as an Indicator of the Chemical Composition and Reactivity

https://doi.org/10.5194/egusphere-2023-403
Preprint. Discussion started: 29 March 2023

of Dissolved Organic Carbon, Environ. Sci. Technol., 37, 4702-4708, https://doi.org/10.1021/es030360x, 2003.

Wen, H., Zhou, Y., Xu, X., Wang, T., Chen, Q., Chen, Q., Li, W., Wang, Z., Huang, Z., Zhou, T., Shi, J., Bi, J., Ji, M., and Wang, X.: Water-soluble brown carbon in atmospheric aerosols along the transport pathway of Asian dust: Optical properties, chemical compositions, and potential sources, Sci. Total Environ., 789, 147971, https://doi.org/10.1016/j.scitotenv.2021.147971, 2021.

Wu, G., Ram, K., Fu, P., Wang, W., Zhang, Y., Liu, X., Stone, E. A., Pradhan, B. B., Dangol, P. M., Panday, A. K., Wan, X., Bai, Z., Kang, S., Zhang, Q., and Cong, Z.: Water-Soluble Brown Carbon in Atmospheric Aerosols from Godavari (Nepal), a Regional Representative of South Asia, Environ. Sci. Technol., 53, 3471-3479, https://doi.org/10.1021/acs.est.9b00596, 2019.

Wu, G., Fu, P., Ram, K., Song, J., Chen, Q., Kawamura, K., Wan, X., Kang, S., Wang, X., Laskin, A., and Cong, Z.: Fluorescence characteristics of water-soluble organic carbon in atmospheric aerosol, Environ. Pollut., 268, 115906, https://doi.org/10.1016/j.envpol.2020.115906, 2021.

Xie, M., Chen, X., Hays, M. D., Lewandowski, M., Offenberg, J., Kleindienst, T. E., and Holder, A. L.: Light Absorption of Secondary Organic Aerosol: Composition and Contribution of Nitroaromatic Compounds, Environ. Sci. Technol., 51, 11607-11616, https://doi.org/10.1021/acs.est.7b03263, 2017.

Xu, J., Hettiyadura, A. P. S., Liu, Y., Zhang, X., Kang, S., and Laskin, A.: Regional Differences of Chemical Composition and Optical Properties of Aerosols in the Tibetan Plateau, J. Geophys. Res.-Atmos., 125, e2019JD031226, https://doi.org/10.1029/2019jd031226, 2020.

Yan, G., and Kim, G.: Speciation and Sources of Brown Carbon in Precipitation at Seoul, Korea: Insights from Excitation-Emission Matrix Spectroscopy and Carbon Isotopic Analysis, Environ. Sci. Technol.,51, 11580-11587, https://doi.org/10.1021/acs.est.7b02892, 2017.

Yu, L., Smith, J., Laskin, A., Anastasio, C., Laskin, J., and Zhang, Q.: Chemical characterization of SOA formed from aqueous-phase reactions of phenols with the triplet excited state of carbonyl and hydroxyl radical, Atmos. Chem. Phys., 14, 13801-13816, https://doi.org/10.5194/acp-14-13801-2014, 2014.

Yu, Q., Chen, J., Qin, W., Cheng, S., Zhang, Y., Sun, Y., Xin, K., and Ahmad, M.: Characteristics, primary sources and secondary formation of water-soluble organic aerosols in downtown Beijing, Atmos. Chem. Phys., 21, 1775-1796, https://doi.org/10.5194/acp-21-1775-2021, 2021.

Yu, X., Yu, Q., Zhu, M., Tang, M., Li, S., Yang, W., Zhang, Y., Deng, W., Li, G., Yu, Y., Huang, Z., Song, W., Ding, X., Hu, Q., Li, J., Bi, X., and Wang, X.: Water Soluble Organic Nitrogen (WSON) in Ambient Fine Particles Over a Megacity in South China: Spatiotemporal Variations and Source Apportionment, J. Geophys. Res.-Atmos., 122, https://doi.org/10.1002/2017jd027327, 2017.

Yue, S., Ren, L., Song, T., Li, L., Xie, Q., Li, W., Kang, M., Zhao, W., Wei, L., Ren, H., Sun, Y., Wang, Z., Ellam, R. M., Liu, C. Q., Kawamura, K., and Fu, P.: Abundance and Diurnal Trends of Fluorescent Bioaerosols in the Troposphere over Mt. Tai, China, in Spring, J. Geophys. Res.-Atmos., 124, 4158-4173, https://doi.org/10.1029/2018jd029486, 2019.

Zeng, Y., Ning, Y., Shen, Z., Zhang, L., Zhang, T., Lei, Y., Zhang, Q., Li, G., Xu, H., Ho, S. S. H., and Cao, J.: The Roles of N, S, and O in Molecular Absorption Features of Brown Carbon in

https://doi.org/10.5194/egusphere-2023-403
Preprint. Discussion started: 29 March 2023

PM2.5 in a Typical Semi‐Arid Megacity in Northwestern China, J. Geophys. Res.-Atmos., 126, e2021JD034791, https://doi.org/10.1029/2021jd034791, 2021.

Zhou, Y., West, C. P., Hettiyadura, A. P. S., Niu, X., Wen, H., Cui, J., Shi, T., Pu, W., Wang, X., and Laskin, A.: Measurement report: Molecular composition, optical properties, and radiative effects of water-soluble organic carbon in snowpack samples from northern Xinjiang, China, Atmos. Chem. Phys., 21, 8531-8555, https://doi.org/10.5194/acp-21-8531-2021, 2021.

Zong, Z., Tian, C., Li, J., Syed, J. H., Zhang, W., Fang, Y., Jiang, Y., Nasir, J., Mansha, M., Rizvi, S. H. H., Shafiq, M., Farhan, S. B., and Zhang, G.: Isotopic Interpretation of Particulate Nitrate in the Metropolitan City of Karachi, Pakistan: Insight into the Oceanic Contribution to NOx, Environ. Sci. Technol., 54, 7787-7797, https://doi.org/10.1021/acs.est.0c00490, 2020.

Zsolnay, A., Baigar, E., Jimenez, M., Steinweg, B., and Saccomandi, F.: Differentiating with fluorescence spectroscopy the sources of dissolved organic matter in soils subjected to drying, Chemosphere, 38, 45-50, https://doi.org/10.1016/S0045-6535(98)00166-0, 1999.